

# CALCIUM ION AS QUANTUM BIT IN A LINEAR PAUL TRAP

Kasim M. Al-Hity

Omdurman Islamic University, Faculty of Engineering Sciences, Dept. of Basic Sciences  
e-mail: kasim68@yahoo.com

## Abstract:

One of the most promising ions to be used as a quantum bit (qubit) is  $^{40}\text{Ca}^+$ . In this paper the effect of the laser wavelength detuning on the quantum register state is studied. Trapped ion quantum computer that was suggested by Cirac is adopted in this work. Starting from laser wavelength 709nm to 749nm, the fidelity is calculated for different physical and geometrical parameters of the linear Paul trap. The two energy levels  $4^2S_{1/2}$  and  $3^2D_{3/2}$  of  $^{40}\text{Ca}^+$  are chosen to represent the two logical states  $|0\rangle$  and  $|1\rangle$  states of the qubit. The results show that the optimum value of the fidelity can be achieved by choosing suitable values of the physical and geometrical parameters. These parameters include the laser incident angle with trap axis, axial trap frequency and Rabi frequency.

## I. Introduction

Quantum computer (QC) is a new device, which is powerful to solve certain important problems efficiently. QC provides massive parallelism by harnessing the exponential nature of quantum mechanics [1] [2]. This *quantum parallelism* is not easy to exploit. However, a few recently discovered quantum algorithms have created a renewed interest in the potential of quantum computation.

The idea of creating computational devices, based on quantum mechanics, was first exploited in 1970's and early of 1980's by physicists and computer scientists such as Charles Bennett, Paul and Richard P. Feynman [1]. The idea emerged when scientists noticed that due to the shrinking of the electronic devices, Moore's law, the size of the electronic systems will reach the size of the atoms or molecules. In that time the rules of the quantum mechanics will be dominant and thus they ask whether a new kind of computer could be devised based on the principles of the quantum mechanics?

Many researchers have shown that QCs can solve some problems more efficiently than the classical one [3] [4] [5]. Obenland [6] studied the effect of two types of the errors on the QC efficiency, inaccuracies and dissipation of the quantum state. The QC model used by Obenland is the one that is suggested by Cirac and Zoller [7]. This model is a string of ions confined in a linear Paul trap as shown in figure 1. Obenland in his work did not study the effect of the variations of the physical and the geometrical parameters. This paper is one of a series of papers to

study the effect of the variations of the physical and geometrical parameters on the quantum register state.

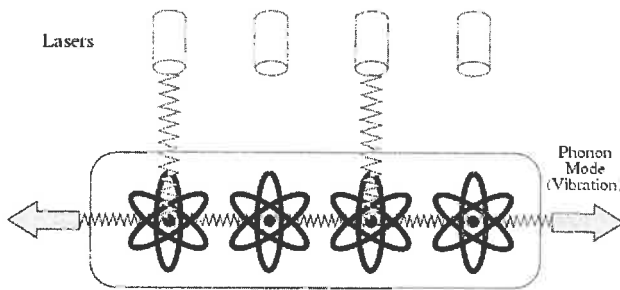


Fig.1 Cirac model for trapped ion QC.

## 2. Theory

### 2.1 Quantum bit and Quantum register

Quantum bit (qubit) represents the basic unit of storage in the QC. It is like a classical one in that it can be in two states, zero or one, but it differs from the classical one in that, because of the properties of quantum mechanics, it can be in both these two states simultaneously [8]. The ket notation of Dirac will be used to represent the qubits.

The qubit that contains both the zero and one values is said to be in the *superposition* of the  $|0\rangle$  and  $|1\rangle$  states. This superposition state persists until the qubit is measured externally. This measurement operation forces the state to be in one of the two values. So that, a register that contains  $M$  qubits can represent  $2^M$  simultaneous values. A calculation performed using this register produces all possible outcomes for  $2^M$  input values thereby obtaining exponential parallelism. Reading out the results of a calculation the qubits have to be measured. This measurement forces all the qubits to a particular value destroying the parallel state.

Because the qubit is a two state system, it can be represented using the two-dimensional complex vector space. Figure 2 shows the representation of a qubit that is in the equal superposition of zero and one. The length of the vector is one because the probabilities of the two possibilities must sum to one. The vector is represented by maintaining the projections upon the  $|0\rangle$  and  $|1\rangle$  states. To create an equal superposition between  $|0\rangle$  and  $|1\rangle$  the vector is rotated (in Hilbert space) half way between  $|0\rangle$  and  $|1\rangle$ . This creates projections  $\cos \frac{\pi}{4} = \sin \frac{\pi}{4} = 1/(\sqrt{2})$  for each of the two states.

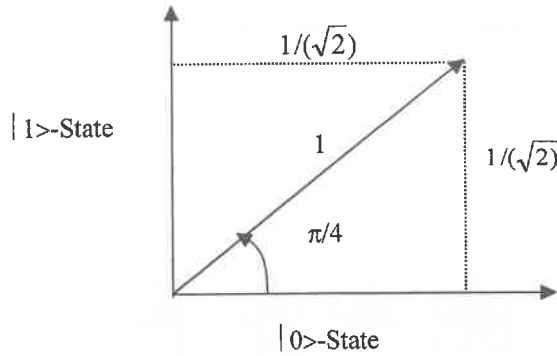


Figure 2. A qubit in the equal superposition state

A *quantum register* of length  $M$  qubit is represented with  $2^M$  dimensional complex vector space [9]. Each string represents a possible bit value of the register. The state of the register ( $\Psi$ ) is therefore a sum of all the possible  $2^M$  vectors, as shown in Equation 1, where each  $\alpha_b$  is a complex number. The squared absolute value of all  $\alpha_b$  values must sum to one. The squared absolute value is formed by calculating the inner product between the vector and its complex conjugate.

$$\Psi = \sum_{b=0}^{2^M-1} \alpha_b |b\rangle \quad , \quad \sum_{b=0}^{2^M-1} \|\alpha_b\|^2 = 1 \quad (1)$$

Here, the following equations show the possible vectors of a two-bit quantum register.

$$|00\rangle = \begin{bmatrix} 1 \\ 0 \\ 0 \\ 0 \end{bmatrix} \quad |01\rangle = \begin{bmatrix} 0 \\ 1 \\ 0 \\ 0 \end{bmatrix} \quad |10\rangle = \begin{bmatrix} 0 \\ 0 \\ 1 \\ 0 \end{bmatrix} \quad |11\rangle = \begin{bmatrix} 0 \\ 0 \\ 0 \\ 1 \end{bmatrix}$$

Each example shows the encoding of a single state, because only one of the  $\alpha_b$  values is non-zero. The  $\alpha_b$  values for a vector that represents an equal superposition state would be non-zero and equal, i.e.  $1/(\sqrt{4})$ .

## 2.2 $^{40}\text{Ca}^+$ Spectroscopy:

One of the most promising and candidate ion to be used as a quantum bit is  $^{40}\text{Ca}^+$ . Figure 3 shows the all energy levels of the  $^{40}\text{Ca}^+$ . The first two terms of the spectroscopic notations (electronic shell quantum number and the multiplicity) are omitted. Five of these transitions (393nm, 397nm, 866nm, 850nm and 854nm) are allowed dipole transitions. While the other two transitions (729nm and 732nm) are quadruples transitions. The levels  $S_{1/2}$  and  $D_{5/2}$  will be associated with the logic states  $|0\rangle$  and  $|1\rangle$  states respectively of a qubit. The optical transition between the two states is an electric quadruple transition. Accordingly, the  $D_{5/2}$  state has a rather long lifetime ( $\approx 1\text{s}$ ) which ensures coherence of the qubit over this time scale [10]. This qubit can be coherently manipulated by a narrow bandwidth laser radiation at 729 nm.

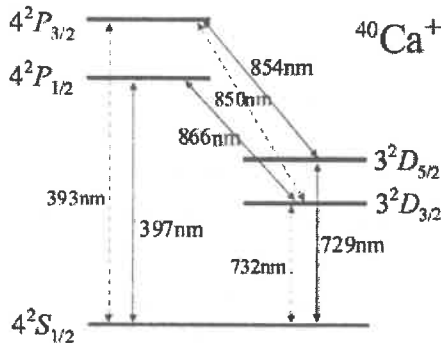


Figure 3. Energy levels diagram of the  $^{40}\text{Ca}^+$ .

### (a) Laser-Ion Interaction:

The Hamiltonian of the interaction of an ion trapped in a harmonic potential of frequency  $\omega$  with the traveling wave of a single mode laser tuned to a transition that forms an effective two-level system is [11]:

$$H = H_0 + H_1 \quad (2)$$

$$H_0 = \frac{p^2}{2m_0} + \frac{1}{2}m_0\omega^2 x^2 + \frac{1}{2}\eta\omega_a\sigma_z \quad (3)$$

$$H_1 = \frac{1}{2}\eta\Omega(\sigma^+ + \sigma^-)(e^{i(kx - \omega t + \phi)} + e^{-i(kx - \omega t + \phi)}) \quad (4)$$

with  $\sigma^+ = \begin{bmatrix} 0 & 1 \\ 0 & 0 \end{bmatrix}$  and  $\sigma^- = \begin{bmatrix} 0 & 0 \\ 1 & 0 \end{bmatrix}$

Where  $k$  is the wave number,  $\omega_l$  the frequency and  $\phi$  the phase of the laser radiation,  $p$  is the linear momentum operator,  $m_0$  is the ion mass,  $\Omega$  is Rabi frequency and  $\sigma_z$  is the Pauli matrix. Here it has assumed that only a single transition ( $\omega_a$  being the atomic transition frequency) is close to resonance and that the laser traveling wave is directed along the x-axis to the ion. Defining the Lamb-Dicke parameter,

$$\eta = k \cos(\alpha) \sqrt{\frac{\hbar}{2m_0\omega}} \quad (5)$$

where  $\alpha$  is the angle between the trap-axis and the laser beam direction. The above expressions of the Hamiltonian in terms of creation and annihilation operators ( $a^+$  and  $a$ ) can be expressed as:

$$H_0 = \hbar\omega(a^+a + \frac{1}{2}) + \frac{1}{2}\hbar\omega_a\sigma_z \quad (6)$$

$$H_1 = \frac{1}{2}\eta\Omega(e^{i\eta(a+a^+)}\sigma^+e^{-i(\omega_l t+\phi)} + e^{-i\eta(a+a^+)}\sigma^-e^{i(\omega_l t+\phi)}) \quad (7)$$

The laser couples the state  $|S, n\rangle$  to all states  $|D, n'\rangle$  where  $n, n'$  are vibration quantum numbers. If the laser is tuned close to resonance of the transition  $|S, n\rangle \leftrightarrow |D, n+m\rangle$  with fixed  $m$  and  $n=0,1,2,3,\dots$  coupling to other levels can be neglected. The transitions which do not change the number of vibration quanta ( $\Delta m = 0$ ) are called carrier transition. A transition is termed blue sideband if an absorption process is accompanied by increase in the motional quantum number ( $\Delta m = +1$ ) while it is termed red sideband if it decreases upon absorption ( $\Delta m = -1$ ).

### (b) Lamb-Dicke Regime

The coupling strengths of a carrier, red and blue sideband as a function of  $n$  can be calculated. This calculation considerably simplifies in the so-called Lamb-Dicke regime defined by the condition ( $\eta^2(2n+1) \ll 1$ ) [6]. The atomic wavepacket, in this regime, is confined to a space much smaller than the wavelength of the atomic transition. Using the first order Taylor expansion in Equation (7):

$$e^{i\eta(a^++a)} = 1 + i\eta(a^+ + a) + O(\eta^2) \quad (8)$$

On the red sideband ( $|S, n\rangle \leftrightarrow |D, n-1\rangle$ ), the Hamiltonian takes the form:

$$H_1 = \frac{1}{2}\eta\Omega(a\sigma^+e^{i\phi} - a^+\sigma^-e^{-i\phi}) \quad (9)$$

### 3. Computational Model

Following Cirac [7] and Obenland [6], Equation (9) can be rewritten as:

$$T(\theta, \phi) = \begin{bmatrix} 1 & 0 & 0 & 0 \\ 0 & \cos(\theta/2) & -ie^{-i\phi} \sin \frac{\theta}{2} & 0 \\ 0 & -ie^{i\phi} \sin \frac{\theta}{2} & \cos(\theta/2) & 0 \\ 0 & 0 & 0 & 1 \end{bmatrix} \quad (10)$$

where  $\theta = \eta\Omega\eta t$ ,  $\phi$  represents the laser phase and  $t$  is the laser pulse time. In our model, the quantum register can be described as

$$\psi = \begin{bmatrix} \frac{1}{2}|S, n-1\rangle \\ \frac{1}{2}|S, n\rangle \\ \frac{1}{2}|D, n-1\rangle \\ \frac{1}{2}|D, n\rangle \end{bmatrix} \quad (11)$$

The standard form of the quantum register can be calculated as  $\psi_s = T(\pi, 0)\psi$ , while the new values of quantum register take the form  $\psi' = T(\theta(\lambda), 0)\psi$ . The fidelity of the quantum register can be calculated as  $\langle \psi_s | \psi' \rangle$ . The fidelity is used as criteria for the agreement between the standard and actual value of the quantum register.

### 4. Results and discussion

The fidelity as a function of laser wavelength is calculated for different physical parameters. The simulation shows that the values of the fidelity near to the unity can be achieved by selecting a complete set of the other parameters. Figure 4 shows the relation between the fidelity as a function of laser wavelength. We start the scanning process from ( $\lambda=709\text{nm}$  to  $\lambda=749\text{nm}$ ). The values of the physical parameters which are used here: Rabi frequency = 150 KHz, the axial trap frequency  $\omega_z = 1\text{MHz}$ , the calcium ion mass  $m=40.08\text{Au}$  and the laser pulse time  $T=5\text{ms}$ . The variation of the laser incident angle  $\alpha$  is starting from  $30^\circ$  to  $80^\circ$ . It is clear that the change in the fidelity values with respect to the change of the incident angle is not linear. The decay from the peak value of the fidelity is rapidly decreased for the small values of laser incident angle. While the deviation from the largest values of the fidelity, is slowly decreasing for the large values of the laser incident angle.

Figure 5 shows the plotting of the fidelity as a function of the laser wavelength with the same parameters of figure 4 using different values of Rabi frequency starting from 100KHz to 500KHz. The value of  $\alpha$  in this figure is  $75^\circ$ . The peak values of the fidelity can be achieved at more than one value of the laser wavelength. As Rabi frequency increased, the peaks positions are shifted towards the small values of the laser wavelength.

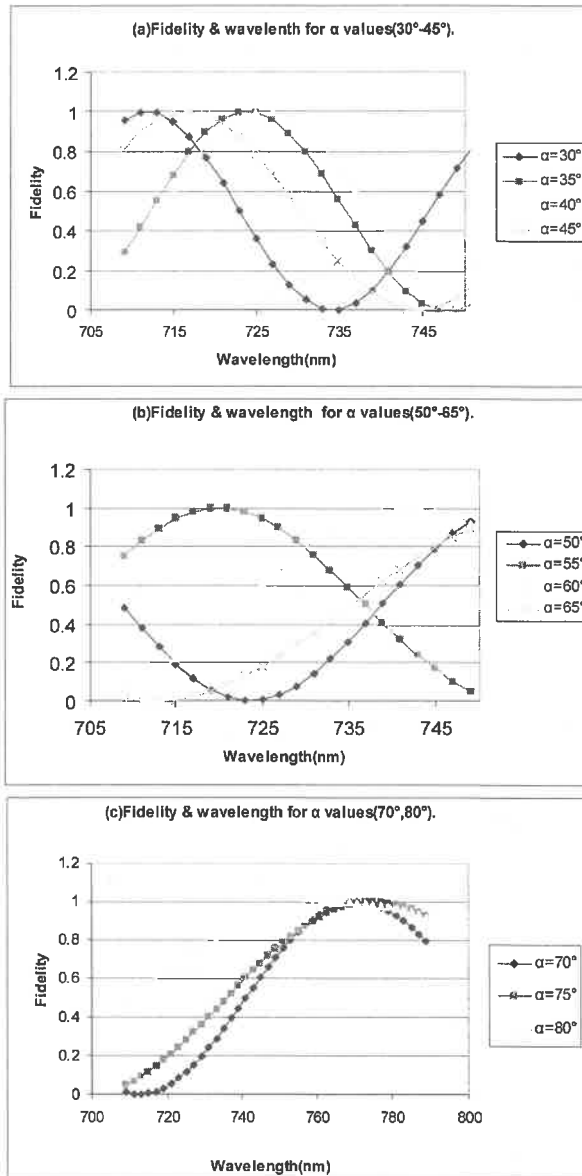
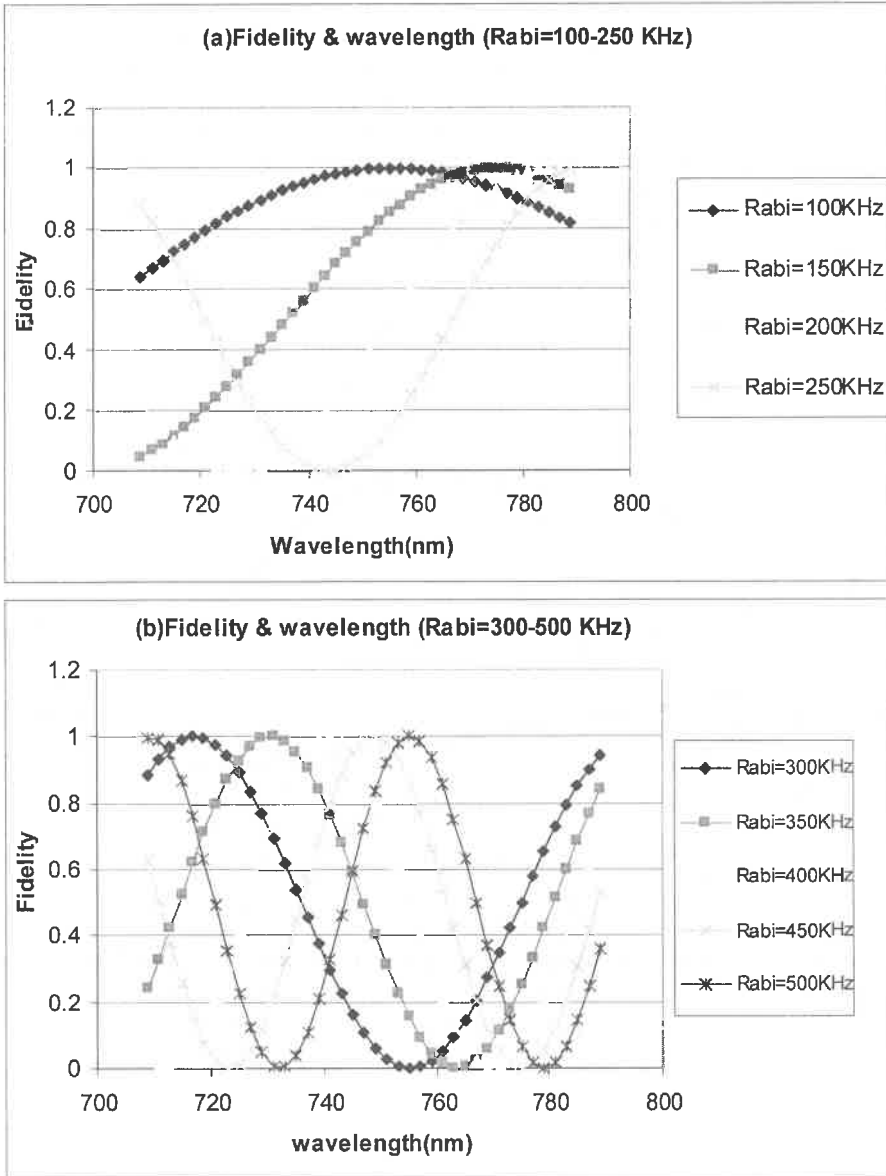


Figure 4. The fidelity as a function of laser wavelength for different values of laser angle  $\alpha$  (a) from (30° to 45°), (b) from (50° to 65°) (c) from (70° to 80°).





The fidelity against the laser wavelength with the same parameters of the previous figures and different values of laser pulse time starting from 1ms to 10ms is plotted in figure 6. While figure 7 shows the relation between the fidelity and the laser wavelength with different values of trap axial frequency  $\omega_z$  starting from 1MHz to 2MHz. The stability of the curves is increasing as the laser pulse time (LPT) increases. The best interval of LPT is  $T=3\text{ms}$  to  $T=8\text{ms}$ . The values of fidelity close to the unity represent the optimum values of the corresponding physical parameters. This goal can be reached by choosing a suitable value of trap frequencies between 1MHz to 2MHz.

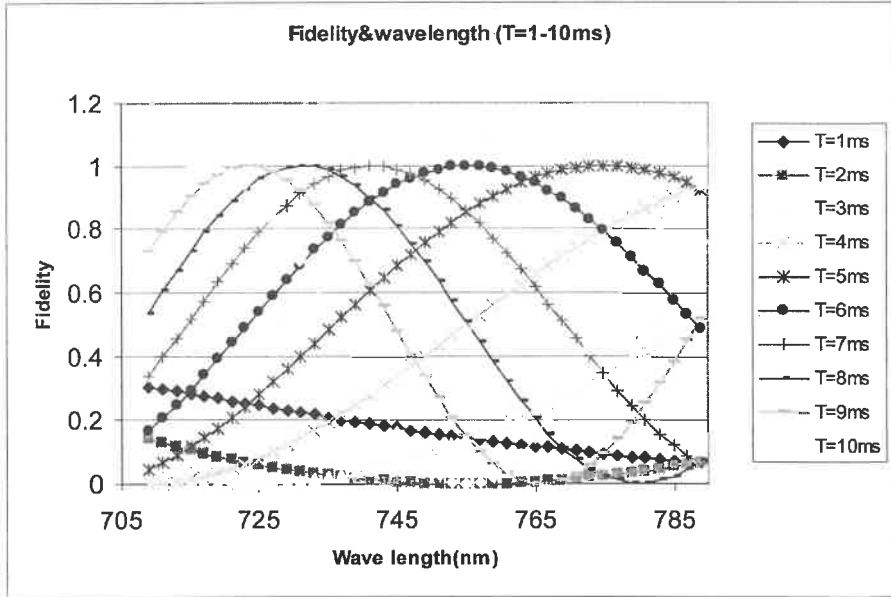


Figure 6. The fidelity as a function of laser wavelength for different values of laser pulse time.

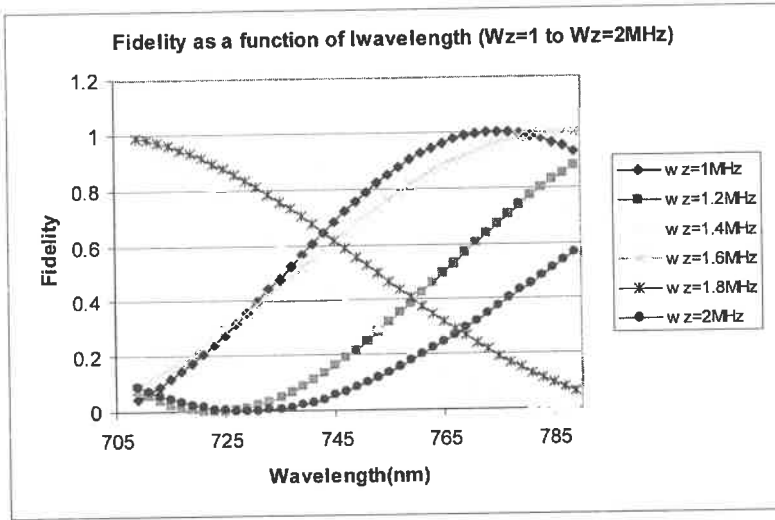


Figure 7. The fidelity as a function of laser wavelength for different values axial trap frequency  $w$ .

### 5. Conclusions

The simulation results show that the operational errors, due to the detuning, affect the fidelity of the quantum register state. The nearest unity value of the fidelity can be achieved in different cases. Choosing a set of suitable values of the geometrical and physical parameters gives the nearest fidelity to one. It is clear from the figures 5-7 that there is a set of optimum values which can be adopted for the trap design and trap operation.

### Acknowledgments

The author would like to thank all the members of Institute of Laser – Sudan University of Science and Technology. My special thanks to Prof. Nefie Abdullateef for his help and advice during the period of the work.

**References:**

- [1] R. Feynman, "Quantum Mechanical Computers" *Foundations of Physics*, 16, No. 6. March 1985.
- [2] P. Benioff. "Quantum Mechanical Models of Turing Machines that Dissipate no Heat". *Physical Review Letters* 48, 1581. 1982.
- [3] I.L. Chuang, R. Laflame, and P.W. Shor, W.H. Zurek. "Quantum Computers, Factoring, and Decoherence ". *Science Vol. 270. December 8, 1995.*
- [4] P. Shor. "Algorithms for Quantum Computation: Discrete Logarithms and Factoring" *Proceedings, 35<sup>th</sup> Annual Symposium on Foundations of Computer Science pp. 124-134. November 1994.*
- [5] M.B. Plenio and P.L. Knight " Realistic Lower Bounds for the Factorization Time of Large Numbers on a Quantum Computer" *Physical Review A* 53, 2986 November 1995.
- [6] K. M. Obenland and A.M. Despain "Simulating the Effect of Decoherence and Inaccuracies on a Quantum Computer" *arXiv:quant-ph/9804038 v1 16 Apr 1998.*
- [7] J. I. Cirac and P. Zoller. "Quantum Computations with Cold Trapped Ions" *Physical Review Letters* 74, Number 20. May 15, pp4091-4096. 1995
- [8] D. Deutsch. "Quantum Theory, the Church-Turing Principle and Universal Quantum Computer" *Proceedings Royal Society London A* 400, pp 97-117. 1985.
- [9] E. Bernstein and U. Vazirani. " Quantum Complexity Theory." in *Proceedings of the 1993 ACM Symposium on the Theory of Computing. ACM Press 1993.*
- [10] H. Haffner, S. Gulde ,M.Riebe, G. Lancaster, C. Becher, J. Eschner, F. Schmidt-Kaler, and R.Blatt "Precision Measurement and Compensation of Optical Stark Shifts for an Io-Trap Quantum Processor" *Physical Rev. Letter Vol.90, Number 14, 2003.*
- [11] J. I. Cirac, A.S. Parkins, R. Blatt, and P. Zoller. "Non-classical state of motion in ion trap" *Adv. Atom. Molec. and Opt. Phys.* 37, 237 (1996).